

Ginzburg-Landau equation bound to the metal-dielectric interface and transverse nonlinear optics with amplified plasmon polaritons

A. Marini and D.V. Skryabin*

Centre for Photonics and Photonic Materials,
Department of Physics,

University of Bath, Bath BA2 7AY, UK

*Corresponding author: d.v.skryabin@bath.ac.uk

(Dated: May 31, 2018)

Using a multiple-scale asymptotic approach, we have derived the complex cubic Ginzburg-Landau equation for amplified and nonlinearly saturated surface plasmon polaritons propagating and diffracting along a metal-dielectric interface. An important feature of our method is that it explicitly accounts for nonlinear terms in the boundary conditions, which are critical for a correct description of nonlinear surface waves. Using our model we have analyzed filamentation and discussed bright and dark spatially localized structures of plasmons.

I. INTRODUCTION

Surface plasmon polaritons (SPPs) are half-photon half-electron surface waves. Thanks to their dual nature, SPPs can be focused tighter than pure light, which is an important property for potential applications in optical processing of information. In the absence of lateral boundaries propagating SPPs are expected to diffract in the interface plane. One way to control diffraction is to structure the surface and make plasmonic waveguides, see, e.g., [1]. Alternatively, one can use nonlinearity for the creation of spatial SPP solitons, which are non-diffracting self-localized surface waves [2, 3]. Other transverse effects with nonlinear plasmons, such as self-focusing and filamentation [4] can be important for frequency conversion, switching and routing experiments with photonics chips. Note, that the interplay between transverse and nonlinear effects have attracted significant attention outside the plasmonics and nanophotonics contexts, see, e.g., [5, 6] for the historic accounts.

Nonlinear functionality of SPPs [7–9] can be significantly hampered by ohmic losses resulting in short propagation distances. One of the possible solutions is to amplify SPPs by doping and pumping the dielectric, so that the losses are either partially or fully compensated [10–12]. The linear dispersion of the amplified SPPs has been studied by several groups, see, e.g., [13, 14]. The linear results have been recently generalized to the more realistic case, when linear gain is nonlinearly saturated above the stimulated emission threshold [15].

Analytical or semi-analytical approaches to describe nonlinear effects with SPPs are very important, since the first principle numerical modelling of nonlinear and multidimensional cases is still computationally demanding. Recently the nonlinear Shrodinger equation (NLS) has been introduced for the plasmons in a slot waveguide formed by two planar metal dielectric interfaces [2] and at a single interface [3]. The *averaging method* implemented in [2, 3] has been borrowed from the theory of the dielectric waveguides [16]. In this approach, one starts from the known solution for the linear SPPs: $\vec{F}(x)e^{i\beta z}$, where

x is the coordinate perpendicular to the interface, z is the propagation direction and β is the propagation constant. Then introducing a slowly varying amplitude $A(z, y)$ and assuming small nonlinearity, the Maxwell equations are averaged in x and the NLS equation for A is derived [2, 3].

The above approach has some drawbacks. First, it is sufficiently well justified only for the quasi-transverse fields, that approximately satisfy the wave equation [16]. Another problem is that it does not treat the boundary conditions rigorously. In particular, continuity of the normal to the interface component of the displacement D_x is guaranteed only in the linear approximation. If the intensity of the guided light peaks away from the interfaces and is small in the proximity of the latter (like it typically happens in dielectric waveguides operating on the principle of total internal reflection), then the nonlinear terms in the boundary conditions can be disregarded. However, the SPP intensity peaks exactly at the interface and nonlinear contribution to the boundary conditions is critical [15, 17]. This is also true for other types of nonlinear surface waves, see, e.g., [18–20].

Thus, it is important to develop a rigorous procedure of deriving the nonlinear evolution equation for surface plasmons, such that the continuity of D_x is enforced together with its nonlinear part. Below we develop a multiple-scale asymptotic approach for the amplified SPPs, which treats the nonlinear boundary conditions rigorously and reveals the differences with the results obtained by the averaging technique. The gain and complex nonlinearity we use are derived using the two-level model. Our procedure leads to the complex Ginzburg-Landau equation that accounts for diffraction of SPPs in the interface plane. The nonlinearity enhancement factor derived by us is intrinsically complex, whilst the averaging approach gives a real one. The difference between the predictions of two approaches increases in the short wavelength limit, where SPPs are maximally localized at the interface, and thus the nonlinear part of the boundary condition is more important. Using our theory we derive a criterion for SPP filamentation and discuss bright and dark spatially localized SPPs. Strictly speaking both soliton families are unstable, though the bright solitons demon-

strate propagation distances sufficient for their practical observation.

II. MODEL

We assume that the interface between metal and dielectric is at $x = 0$ and z, y are the in-plane coordinates. The evolution of SPPs obeys the time independent Maxwell equations

$$\partial_{xy}^2 E_y - \partial_{yy}^2 E_x - \partial_{zz}^2 E_x + \partial_{zx}^2 E_z = \epsilon E_x, \quad (1)$$

$$\partial_{yz}^2 E_z - \partial_{zz}^2 E_y - \partial_{xx}^2 E_y + \partial_{xy}^2 E_x = \epsilon E_y, \quad (2)$$

$$\partial_{xz}^2 E_x - \partial_{xx}^2 E_z - \partial_{yy}^2 E_z + \partial_{zy}^2 E_y = \epsilon E_z. \quad (3)$$

The coordinates are dimensionless and normalized to the inverse wavenumber $k = 2\pi/\lambda_{vac}$, where λ_{vac} is the vacuum wavelength. The permittivity on the dielectric side of the interface ($x > 0$) is

$$\epsilon = \epsilon_d + \chi(|E_x|^2 + |E_y|^2 + |E_z|^2), \quad (4)$$

$$\epsilon_d = \epsilon'_d + i\epsilon''_d, \quad \chi = \chi' + i\chi''. \quad (5)$$

The permittivity on the metal side ($x < 0$) is

$$\epsilon = \epsilon_m = \epsilon'_m + i\epsilon''_m. \quad (6)$$

If SPPs are amplified by means of active inclusions in the dielectric, then ϵ_d and χ are functions of the gain coefficient α . The propagation constant β for linear plasmons is

$$\beta = \sqrt{\epsilon_d \epsilon_m / (\epsilon_d + \epsilon_m)}. \quad (7)$$

where β becomes real at the threshold: $\alpha = \alpha_0$ [13]:

$$\beta(\alpha_0) \equiv \beta_0, \quad \text{Im}\beta_0 = 0. \quad (8)$$

The linear and nonlinear permittivities for the dielectric at $\alpha = \alpha_0$ are $\epsilon_d(\alpha_0) = \epsilon_{d0}$ and $\chi(\alpha_0) = \chi_0$.

The active inclusions are approximated by the 2-level atom susceptibility. For light intensities much smaller than the transition saturation intensity I_s we find [15, 21]

$$\epsilon_d = \epsilon_b - \alpha \frac{i - \delta}{1 + \delta^2}, \quad (9)$$

$$\chi = \alpha \frac{i - \delta}{(1 + \delta^2)^2}. \quad (10)$$

where ϵ_b is the real dielectric constant of the background material hosting the two-level atoms. $\delta = (\omega - \omega_a)T_2$ is the dimensionless detuning from the atomic resonance frequency, $\omega_a = 2\pi c/\lambda_a$, normalized to the transition linewidth, T_2^{-1} . α is the dimensionless gain coefficient at the line center. The electric field is normalized to $\sqrt{I_s}$, which implies that the nonlinear susceptibility χ is dimensionless, see [15] for more details. Possible dependence of the atomic life times from the distance to

the interface, see, e.g., [22], are specific to a choice of a pumping technique and are disregarded in what follows.

The threshold gain α_0 works out as

$$\alpha_0(\omega) = \frac{1}{2\epsilon''_m} \left(|\epsilon_m|^2 - 2\epsilon''_m \epsilon_b \delta \right) \pm \frac{1}{2\epsilon''_m} \sqrt{|\epsilon_m|^4 - 4\epsilon''_m \epsilon_b \left(\epsilon''_m \epsilon_b + \delta |\epsilon_m|^2 \right)}. \quad (11)$$

Lossless propagation of SPPs is impossible above the critical value of $\delta = \delta_{lim}$ as determined by the condition that the square root in Eq. (11) becomes zero. At this point, the two solutions for α_0 degenerate, see Fig. 1. δ_{lim} should not be confused with the plasmon resonance frequency, δ_{spp} , which corresponds to the zero of the denominator of β_0 . The existence boundaries of the SPPs at $\alpha = \alpha_0$ are determined by either or both of δ_{lim} and δ_{spp} , see Fig. 1. The upper branch solution (dashed lines in Fig. 1) corresponds to high gain coefficients implying refractive indices of order 10 or larger. In our subsequent numerical examples we focus on relatively small $|\delta|$'s, thereby selecting the lower branch of α_0 (minus sign in front of the square root in Eq. (11)). This branch corresponds to relatively small changes of the background refractive index as achievable for small densities of active atoms [14]. Note, that ϵ_m is frequency dependent, i.e., $\epsilon_m(\omega) = \epsilon_m(\delta/T_2 + \omega_a)$. Hence α_0 is a function of both δ and ω_a . We choose silver as a metal in all our calculations.

III. FIRST PRINCIPLE DERIVATION OF THE GINZBURG-LANDAU EQUATION FOR SPPS

The perturbation theory developed below assumes relatively small deviations of the gain coefficient from its threshold value α_0 , i.e.

$$\alpha - \alpha_0 \equiv \alpha_0 g, \quad |g| \ll 1. \quad (12)$$

The ansatz for the field components in the dielectric and metal is

$$\begin{aligned} E_{x,j} &= \left[A_{x,j}^{(0)} + A_{x,j}^{(1)} + O(|g|^{5/2}) \right] e^{i\beta_0 z}, \\ E_{y,j} &= \left[A_{y,j}^{(0)} + O(|g|^2) \right] e^{i\beta_0 z}, \\ E_{z,j} &= \left[A_{z,j}^{(0)} + A_{z,j}^{(1)} + O(|g|^{5/2}) \right] e^{i\beta_0 z}, \quad j = d, m \end{aligned} \quad (13)$$

where $A_{x,j}^{(0)} \sim |g|^{1/2}$, $A_{x,j}^{(1)} \sim |g|^{3/2}$, $A_{y,j}^{(0)} \sim |g|$, $A_{z,j}^{(0)} \sim |g|^{1/2}$, and $A_{z,j}^{(1)} \sim |g|^{3/2}$. All A 's are the functions of z, y and x . However, their dependencies on z and y are assumed slow relative to the fast oscillations of $e^{i\beta_0 z}$:

$$\partial_y \sim |g|^{1/2}, \quad \partial_z \sim |g|. \quad (14)$$

Though the y component deviates from zero, when the field has finite size along y , it is expected to remain relatively small, $\sim |g|$.

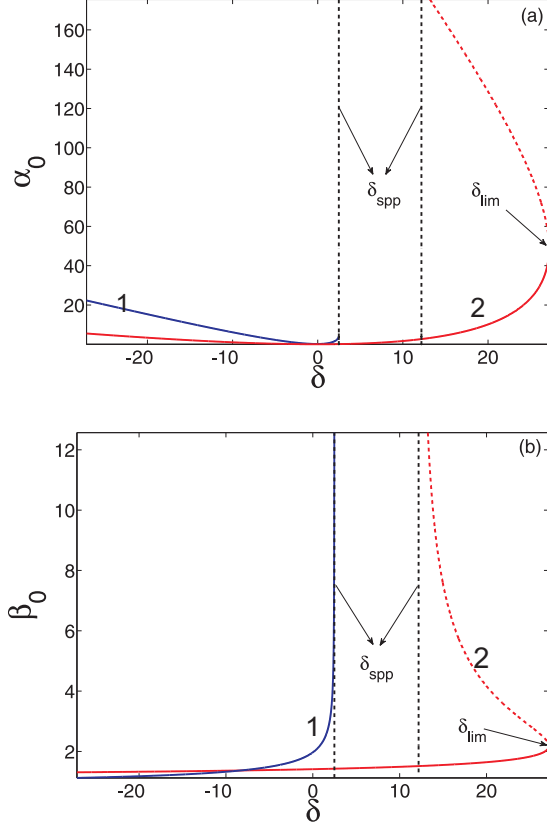


FIG. 1: (Color online) (a) Threshold gain α_0 vs detuning δ for two different atomic resonances: $\lambda_a = 400\text{nm}$ (line 1 (blue)) and $\lambda_a = 700\text{nm}$ (line 2 (red)). (b) β_0 vs δ . Parameters and notations as in a). The full/dashed line corresponds to the minus/plus in Eq. (11).

The dielectric susceptibility is trivially expanded into the g -series:

$$\epsilon_d = \epsilon_{d0} + \epsilon_{d1}, \quad \epsilon_{d1} \equiv g\alpha_0\partial_\alpha\epsilon_d. \quad (15)$$

The only value of the nonlinear coefficient χ , we require below is the one taken exactly at the threshold $\chi(\alpha_0) \equiv \chi_0$.

A. $|g|^{1/2}$ and $|g|^1$ orders

By substituting Eqs. (13) into the Maxwell equations, we find in the order $|g|^{1/2}$

$$\hat{M}_j \begin{bmatrix} A_{x,j}^{(0)} \\ A_{z,j}^{(0)} \end{bmatrix} = 0, \quad j = d, m. \quad (16)$$

Here

$$\hat{M}_j = \begin{pmatrix} q_j^2 & i\beta_0\partial_x \\ 0 & \partial_{xx}^2 - q_j^2 \end{pmatrix} \quad (17)$$

and

$$q_d^2 = \beta_0^2 - \epsilon_{d0}, \quad q_m^2 = \beta_0^2 - \epsilon_m. \quad (18)$$

Any nonlinear and transverse, i.e., y -dependent, effects are disregarded in Eq. (16).

The SPP solution of Eq. (16) is well known:

$$\begin{aligned} A_{x,d}^{(0)} &= \frac{i\beta_0}{q_d} A(y, z) e^{-q_d x}, \\ A_{z,d}^{(0)} &= A(y, z) e^{-q_d x}, \\ A_{x,m}^{(0)} &= -\frac{i\beta_0}{q_m} A(y, z) e^{q_m x}, \\ A_{z,m}^{(0)} &= A(y, z) e^{q_m x}. \end{aligned} \quad (19)$$

Eqs. (19) satisfy continuity of the normal component of the displacement and tangential components of the field: $\epsilon_d A_{x,d}^{(0)} = \epsilon_m A_{x,m}^{(0)}$ and $A_{z,m}^{(0)} = A_{z,d}^{(0)}$ at $x = 0$. The former condition implies $\epsilon_{d0} q_m = -\epsilon_m q_d$ giving (after some algebra) the expression for β_0 , see Eq. (7).

In the order $|g|^1$, we find the linear equations for the y component of the field

$$q_j^2 A_{y,j}^{(0)} - \partial_{xx}^2 A_{y,j}^{(0)} = 0, \quad (20)$$

which are readily solved

$$\begin{aligned} A_{y,d}^{(0)} &= B(y, z) e^{-q_d x} \\ A_{y,m}^{(0)} &= B(y, z) e^{q_m x}. \end{aligned} \quad (21)$$

To determine the unknown functions $A(y, z)$ ($|A| \sim |g|^{1/2}$) and $B(y, z)$ ($|B| \sim |g|$) we need to proceed to the higher orders of our perturbation series.

B. $|g|^{3/2}$ order and Ginzburg-Landau equation

Proceeding to the order $|g|^{3/2}$, we find an inhomogeneous system of differential equations for corrections to the standard SPP solutions. The correction equations on the metal side are

$$\hat{M}_m \begin{bmatrix} A_{x,m}^{(1)} \\ A_{z,m}^{(1)} \end{bmatrix} = \begin{bmatrix} K_x \\ K_z \end{bmatrix} e^{q_m x}, \quad (22)$$

where

$$\begin{aligned} K_x &= \frac{\beta_0^2 + \epsilon_m}{q_m} \partial_z A - q_m \partial_y B - \frac{i\beta_0}{q_m} \partial_{yy}^2 A, \\ K_z &= -2i\beta_0 \partial_z A - \partial_{yy}^2 A. \end{aligned}$$

A solution of Eqs. (22) consists of a particular solution of the inhomogeneous problem plus a general solution of the corresponding homogeneous system ($K_{x,z} = 0$):

$$\begin{aligned} A_{x,m}^{(1)} &= \frac{1}{2q_m^3} [-i\beta_0 K_z (1 + q_m x) + 2q_m K_x] e^{q_m x} \\ &\quad - c \frac{i\beta_0}{q_m} e^{q_m x} \\ A_{z,m}^{(1)} &= \frac{K_z}{2q_m} x e^{q_m x} + c e^{q_m x}, \end{aligned} \quad (23)$$

where c is a constant to be determined from the boundary conditions.

The righthand sides of the corresponding equations in the dielectric are more cumbersome due to nonlinear terms:

$$\hat{M}_d \begin{bmatrix} A_{x,d}^{(1)} \\ A_{z,d}^{(1)} \end{bmatrix} = \quad (24)$$

$$e^{-q_d x} \left\{ \begin{bmatrix} L_x \\ L_z \end{bmatrix} + \begin{bmatrix} N_x \\ N_z \end{bmatrix} e^{-2x \text{Re} q_d} \right\},$$

where

$$L_x = -\frac{1}{q_d} (\beta_0^2 + \epsilon_{d0}) \partial_z A + \frac{i\beta_0}{q_d} \epsilon_{d1} A + q_d \partial_y B + \frac{i\beta_0}{q_d} \partial_{yy}^2 A$$

$$L_z = -2i\beta_0 \partial_z A - \epsilon_{d1} A - \partial_{yy}^2 A$$

$$N_x = \frac{i\beta_0}{q_d} \left(\frac{\beta_0^2}{|q_d|^2} + 1 \right) \chi_0 |A|^2 A$$

$$N_z = -\frac{(\epsilon_{d0} q_d + 2\beta_0^2 \text{Re} q_d) (|q_d|^2 + \beta_0^2)}{\epsilon_{d0} q_d |q_d|^2} \chi_0 |A|^2 A.$$

Solutions of Eqs. (24) are given by

$$A_{x,d}^{(1)} = \frac{1}{2q_d^3} [i\beta_0 L_z (1 - q_d x) + 2q_d L_x] e^{-q_d x} \quad (25)$$

$$+ \frac{1}{q_d^2} \left[N_x + \frac{i\beta_0 N_z (2\text{Re} q_d + q_d)}{4\text{Re} q_d (\text{Re} q_d + q_d)} \right] e^{-2\text{Re} q_d x - q_d x}$$

$$A_{z,d}^{(1)} = \left[-\frac{L_z}{2q_d} x + \frac{N_z e^{-2\text{Re} q_d x}}{4\text{Re} q_d (\text{Re} q_d + q_d)} \right] e^{-q_d x}.$$

The arbitrary constant terms in Eqs. (25) have been omitted, as this does not lead to any loss of generality.

Combining Eqs. (19),(21),(23),(25) with Eqs. (13) and substituting the calculated fields into the boundary conditions

$$[\epsilon_d + \chi(|E_{x,d}|^2 + |E_{y,d}|^2 + |E_{z,d}|^2)] E_{x,d} = \epsilon_m E_{x,m}, \quad (26)$$

$$E_{z,m} = E_{z,d}, \quad E_{y,m} = E_{y,d},$$

we find that the latter are satisfied in the order $|g|^{3/2}$ only providing that

$$c = \frac{N_z}{4(q_d + \text{Re} q_d) \text{Re} q_d} \quad (27)$$

and the amplitude A solves the complex Ginzburg-Landau equation

$$2i\beta_0 \partial_z A + \partial_{yy}^2 A + f A + \gamma |A|^2 A = 0, \quad (28)$$

where

$$f \equiv g \frac{\alpha_0 \epsilon_m^2 \partial_\alpha \epsilon_d}{(\epsilon_{d0} + \epsilon_m)^2},$$

$$\gamma \equiv h \chi_0, \quad h \equiv \frac{\beta_0^4}{\epsilon_{d0}^2} \frac{q_d (|q_d|^2 + \beta_0^2)}{(q_d + \text{Re} q_d) |q_d|^2}.$$

All the terms containing $B(y, z)$ cancel out leaving this function undetermined until the higher order corrections are accounted for. Thus taking the plasmonic field as in Eqs. (13) with the amplitude A obeying Eq. (28) we are guaranteed that the nonlinear boundary conditions are satisfied upto and including the $|g|^{3/2}$ -terms.

The first and second terms in Eq.(28) describe the propagation and diffraction of SPPs. $\text{Re} f$ accounts for the shift of the propagation constant away from β_0 , when gain deviates from the threshold. $\text{Im} f$ accounts for the gain excess ($\alpha > \alpha_0$, $\text{Im} f < 0$) or shortage ($\alpha < \alpha_0$, $\text{Im} f > 0$). The nonlinear term provides an additional shift of the propagation constant ($\text{Re} \gamma |A|^2$) and of the nonlinear loss ($\text{Im} \gamma |A|^2$) that counterbalances the linear gain. Note, that the transformation back to physical units results in the appearance of a k^2 factor in the 3rd and 4th terms of Eq. (28).

C. Comparison with the averaging approach

Parameter h in the expression for γ is the nonlinearity enhancement factor. h accounts for the difference between the nonlinear responses of SPPs and free waves propagating far from the interface. h is complex, therefore, even when atomic nonlinearity is purely dispersive or purely absorptive, the effective SPP nonlinearity is a mixture of both types. This contrasts results using the averaging approach [2, 3, 16], where h is real.

The averaging approach yields a well known expression for the effective nonlinearity of guided modes. Following this method, one should replace h in Eq. (28) with \tilde{h} [2, 3]

$$\tilde{h} = \frac{\int_0^{+\infty} dx |\vec{F}|^4}{\int_{-\infty}^{+\infty} dx |\vec{F}|^2} \quad (29)$$

Here \vec{F} is the plasmonic field given by Eq. (19) with $A = 1$.

We fix the detuning and plot h and \tilde{h} as functions of the resonance wavelength, λ_a in Fig. 2. On the short wavelength side the plots in Fig. 2 are limited by the zero of the denominator of β_0 . Through this it is seen that the two approaches give qualitatively similar dependencies in the long wavelength limit, whilst in the short wavelength limit, our calculations predict a significantly higher nonlinearity enhancement. Physically, one can identify two factors determining changes in h with the resonance wavelength. Tendency for $\text{Re} h$ and \tilde{h} to decrease with decreasing λ_a is linked to the fact that SPP intensity on the metal side increases relative to the intensity on the dielectric side, as wavelength decreases. Since the metal is linear in our model, it should lead to a drop in the nonlinearity enhancement coefficient. However the smaller wavelengths reaching the SPP resonance imply that the SPP field profile is getting squeezed closer to the interface on both sides and therefore the nonlinear

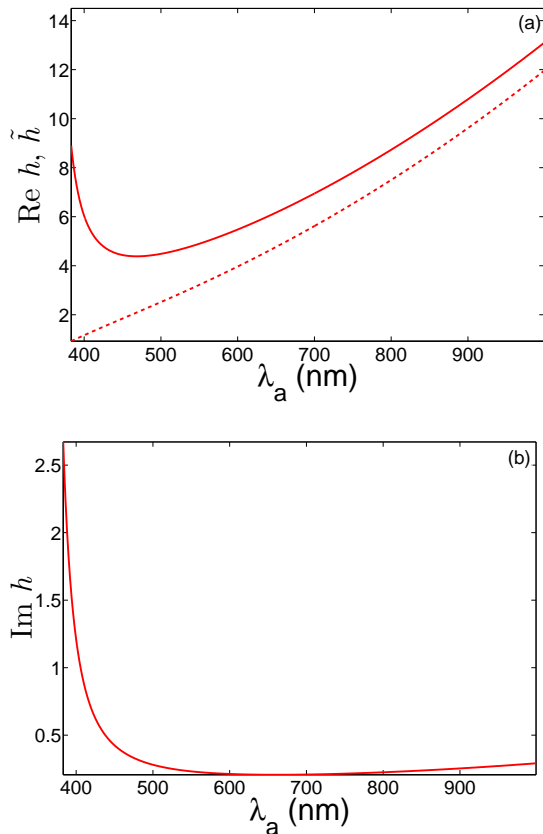


FIG. 2: (Color online) (a) Nonlinearity enhancement coefficients $\text{Re}h$ (full line) and \tilde{h} (dashed line) calculated using two different approaches vs λ_a . (b) $\text{Im}h$. Varying δ inside the transition linewidth leads only to small difference in h . The graphs shown correspond to $\delta = -0.5$. The short wavelength boundary of the both plots corresponds to the point where β_0 becomes imaginary.

part of the boundary conditions becomes more important. This makes the difference between $\text{Re}h$ and \tilde{h} , and the deviation of $\text{Im}h$ from zero pronounced in the short wavelength limit, see Fig. 2.

IV. FILAMENTATION AND TRANSVERSELY LOCALIZED SPPS

A. Filamentation of SPPs

The plane wave solution of Eq. (28) is

$$A_0 = \rho \times \exp \left[i \frac{z}{2\beta_0} (\text{Re}f - \rho^2 \text{Re}\gamma) \right], \quad (30)$$

$$\rho^2 = -\frac{\text{Im}f}{\text{Im}\gamma} > 0.$$

$-\text{Im}f > 0$ implies the gain above threshold, i.e., $\alpha > \alpha_0$. $\text{Im}\gamma > 0$ implies absorptive nonlinearity compensating

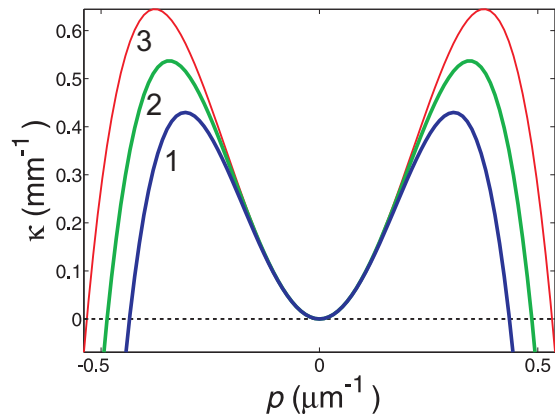


FIG. 3: (Color online) Growth rate κ of the filamentation instability expressed in physical units as a function of momentum p . $\lambda_a = 594 \text{ nm}$, $\delta = -0.3$, $\alpha_0 = 0.0063$ and $g = 0.4, 0.5, 0.6$ for blue (line 1), green (line 2) and red (line 3) curves respectively.

for the excess gain. Together these conditions lead to the existence of the SPP solution with the constant stationary amplitude, ρ . The expression for ρ , however, diverges and our approach breaks down if the nonlinear absorption becomes zero, i.e. $\text{Im}\gamma = 0$. This critical case requires one to account for quintic nonlinear terms in the perturbation expansion, which goes beyond our present objectives.

The solution (30) can be unstable with respect to a pattern forming filamentation instability, as known for the generic Ginzburg-Landau equation [23]. In order to study the stability problem we perturb A_0 with small amplitude waves carrying transverse momentum p :

$$A = (1 + q_+ e^{\kappa z + ipy} + q_-^* e^{\kappa^* z - ipy}) A_0. \quad (31)$$

Inserting Eq.(31) into Eq.(28) and linearizing for small $|q_{\pm}|$ we find two solutions for κ . The unstable one is given by:

$$2\beta_0 \kappa = \text{Im}f + \sqrt{\text{Im}^2 f - p^2(p^2 - 2p_{max}^2)}. \quad (32)$$

The filamentation instability sets in providing $\text{Re}\kappa > 0$. In Fig. 3, it is seen that the $\text{Re}\kappa$ vs p plot has the typical two peak shape. The maximal instability growth rate is achieved for

$$p = \pm p_{max}, \quad p_{max}^2 \equiv \rho \text{Re}\gamma. \quad (33)$$

The characteristic filament size in physical units is $w \approx \lambda_{vac}/p_{max}$. w as a function of λ_a is plotted in Fig. 4.

The instability domain in the (δ, α) -plane is shown in Fig. 5. Filamentation is present for the self-focusing effective nonlinearity, i.e., $\text{Re}\gamma > 0$. If the nonlinearity enhancement factor is real, then $\text{Re}\gamma = 0$ simply implies $\text{Im}\chi = 0$, which is achieved at the line center $\delta = 0$. In this case, the nonlinearity changes from focusing (filamentation) to defocusing (no filamentation) at

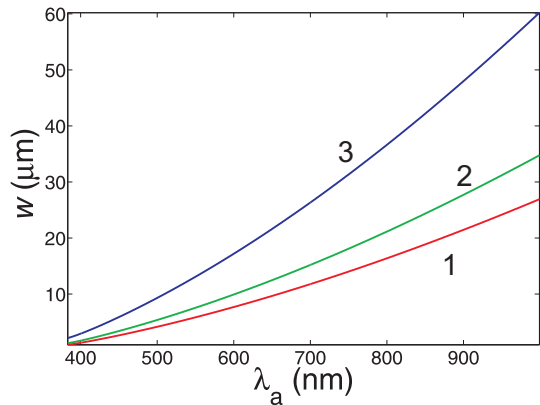


FIG. 4: (Color online) The characteristic filament size w scaled back into physical units vs λ_a for $\delta = -0.5$, $g = 0.1, 0.3, 0.5$ for blue (line 3), green (line 2) and red (line 1) curves respectively.

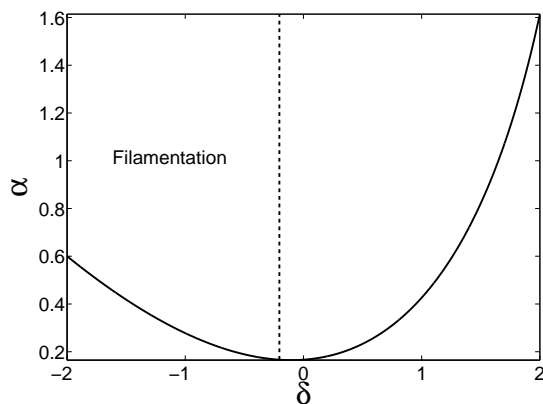


FIG. 5: Lossless SPPs exist above the full line corresponding to $\alpha = \alpha_0$. SPPs are unstable with respect to filamentation on the left from the dashed vertical line, corresponding to $\text{Re}\gamma = 0$. $\lambda_a = 400 \text{ nm}$.

the atomic resonance, i.e. exactly as in the bulk material. However, the fact that $\text{Im}h \neq 0$ leads to the offset of the instability boundary away from $\delta = 0$, see Fig. 5. Gain values corresponding to approximately 50% above threshold imply the development of a filamentary pattern over distances of 1 – 3mm.

B. Bright and dark localized SPPs

The cubic Ginzburg-Landau equation is known to have a wide variety of localised solutions, which can be relevant in the SPP context under different circumstances. Detailed classification of these solutions can be found in, e.g., Refs. [23, 24]. Here we briefly introduce the most ubiquitous of those, which are bright Pereira-Stenflo [25] and dark Nozaki-Bekki [26] localised solutions.

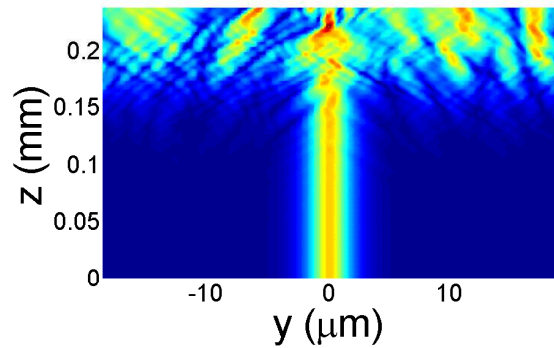


FIG. 6: (Color online) Propagation of a bright localized solution and instability of its background: $\lambda_a = 594 \text{ nm}$, $\delta = -0.3$, $\alpha = 0.0183$, $\alpha_0 = 0.0063$.

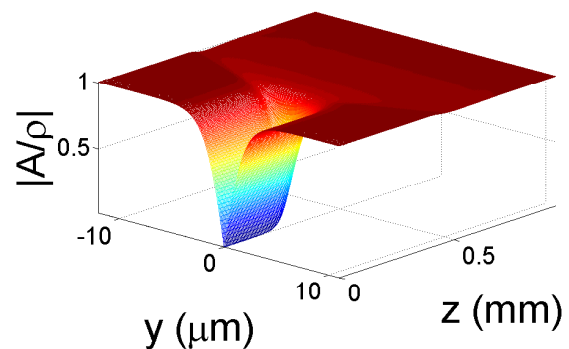


FIG. 7: (Color online) Destabilization of the dark soliton due to core instability: $\lambda_a = 594 \text{ nm}$, $\delta = -0.3$, $\alpha = 0.0183$, $\alpha_0 = 0.0063$.

Both bright and dark localised solutions exist under the same conditions: $\text{Im}f < 0$ (positive gain) and $\text{Im}\gamma > 0$ (nonlinear absorption). The bright solution is given by

$$A(y, z) = \rho \sqrt{\frac{3}{2}} [\text{sech}(Ky)]^{1+ia} \exp(iuz), \quad (34)$$

and the dark one by

$$A(y, z) = \rho \frac{\tanh(sy)}{[\cosh(sy)]^{ib}} \exp(ivz). \quad (35)$$

Explicit expressions for the parameters entering Eqs. (34), (35) are given in the Appendix. In the limit $|y| \rightarrow \infty$ the dark solution tends towards the plane wave solution (30).

The bright solution is unstable because its zero background is unstable above threshold. This instability is relatively slow to develop and practical observation of bright solitons over distances of 100s of microns is still possible, see numerical modelling results in Fig. 6. The dark solution is known to be unstable with respect to the core instability through most of its existence domain, see, e.g., [27], which is complemented by the filamentation of

background, provided the effective Kerr nonlinearity is self-focusing. Fig. 7 shows an example of the core instability, where one can see that for the chosen parameters it develops over the shorter distance, if compared to the instability of the zero background of the bright solution in Fig. 6.

V. SUMMARY

We have considered nonlinear propagation of the amplified and diffracting surface plasmon polaritons above the threshold beyond which the plasmon propagation constant becomes real. Starting from the first principle Maxwell equations, we have developed a technique allowing derivation of the complex cubic Ginzburg-Landau equation for the slowly varying plasmon amplitude. The nonlinear plasmon solutions found by our method is guaranteed to satisfy nonlinear boundary conditions at the interface to the required accuracy. This distinguishes our approach and results from the recently proposed derivation of the nonlinear Schrödinger equation for surface plasmons, which satisfy boundary conditions only in the linear approximation [2, 3]. We have found that the nonlinearity enhancement factor is always complex and hence mixes real and imaginary parts of the intrinsic nonlinearity of a dielectric. This mixing changes conditions required for the filamentation of plasmons and the existence of the dark (Nozaki-Bekki) and bright (Pereira-Stenflo) spatially localized waves, relative to the respective conditions in bulk medium. Though both of the localized solutions are unstable with respect to growth of small perturbations, the bright ones demonstrate quasi-stable propagation over the distances of 100's of microns and are likely to be practically observable. Finding mech-

anisms leading to stabilization of these structures is an important topic for future research.

VI. ACKNOWLEDGEMENT

We acknowledge useful discussions with A. Gorbach, A. Zayats.

Appendix

The parameters entering Eq. (34) are expressed in terms of the parameters for the Ginzburg-Landau equation Eq. (28) as

$$a = -\frac{3\text{Re}\gamma}{2\text{Im}\gamma} + \sqrt{2 + \left(\frac{3\text{Re}\gamma}{2\text{Im}\gamma}\right)^2},$$

$$K^2 = -\frac{1}{2a}\text{Im}f,$$

$$u = \frac{1}{2\beta_0}\text{Re}f + \frac{a^2 - 1}{4\beta_0 a}\text{Im}f.$$

Parameters entering Eq. (35) are

$$b = -\frac{3\text{Re}\gamma}{2\text{Im}\gamma} - \sqrt{2 + \left(\frac{3\text{Re}\gamma}{2\text{Im}\gamma}\right)^2},$$

$$s^2 = \frac{1}{3b}\text{Im}f,$$

$$v = \frac{1}{2\beta_0}\text{Re}f - \frac{1}{3b\beta_0}\text{Im}f.$$

-
- [1] S. I. Bozhevolnyi, V. S. Volkov, E. Devaux, J. Y. Laluet, and T. W. Ebbesen, *Nature* **440**, 508 (2006).
 - [2] E. Feigenbaum and M. Orenstein, *Opt. Lett.* **32**, 674 (2007).
 - [3] A. R. Davoyan, I. V. Shadrivov, and Y. S. Kivshar, *Opt. Express* **17**, 21732 (2009).
 - [4] Y. Y. Lin, R. K. Lee, and Y. S. Kivshar, *Opt. Lett.* **34**, 2982 (2009).
 - [5] N. B. Abraham and W. J. Firth, *J. Opt. Soc. Am. B* **7**, 951 (1990).
 - [6] Y. Kivshar and G. Agrawal, *Optical Solitons: From Fibers to Photonic Crystals* (Academic Press, 2003).
 - [7] G. A. Wurtz, R. Pollard, and A. V. Zayats, *Phys. Rev. Lett.* **97**, 057402 (2006).
 - [8] D. Pacifici, H. J. Lezec, and H. A. Atwater, *Nature Photonics* **1**, 402 (2007).
 - [9] K. F. MacDonald, Z. L. Samson, M. I. Stockman, and N. I. Zheludev, *Nature Photonics* **3**, 55 (2009).
 - [10] G. Winter, S. Wedge, and W. L. Barnes, *New J. Phys.* **8**, 125 (2006).
 - [11] M. A. Noginov, G. Zhu, M. Mayy, B. A. Ritzo, N. Nogi-nova, and V. A. Podolskiy, *Phys. Rev. Lett.* **101**, 226806 (2008).
 - [12] A. Ambati, S. H. Nam, E. Ulin-Avila, A. Genov, G. Bartal, and X. Zhang, *Nano Letters* **8**, 3998 (2008).
 - [13] M. P. Nezhad, K. Tetz, and Y. Fainman, *Opt. Express* **12**, 4072 (2004).
 - [14] M. A. Noginov, V. A. Podolskiy, G. Zhu, M. Mayy, M. Bahoura, J. A. Adegoke, B. A. Ritzo, and K. Reynolds, *Opt. Express* **16**, 1385 (2008).
 - [15] A. Marini, A. V. Gorbach, D. V. Skryabin, and A. V. Zayats, *Opt. Lett.* **34**, 2864 (2009).
 - [16] G. P. Agrawal, *Nonlinear Fiber Optics* (Academic press, 2001).
 - [17] D. Mihalache, G. I. Stegeman, C. T. Seaton, E. M. Wright, R. Zononi, A. D. Boardman, and T. Twardowski, *Opt. Lett.* **12**, 187 (1987).
 - [18] V. M. Agranovich, V. Babichenko, and Y. Chernyak, *Sov. Phys. JETP Lett.* **32**, 512 (1980).
 - [19] A. D. Boardman, G. S. Cooper, A. A. Maradudin, and T. P. Shen, *Phys. Rev. B* **34**, 8273 (1986).
 - [20] J. Moloney and A. Newell, *Nonlinear Optics* (Addison-Wesley, 1992).
 - [21] R. W. Boyd, *Nonlinear Optics* (Academic Press, 2003).

- [22] I. De Leon and P. Berini, *Physical Review B* **78**, 161401 (2008).
- [23] I. S. Aranson and L. Kramer, *Rev. Mod. Phys.* **74**, 99 (2002).
- [24] N. Akhmediev and A. Ankiewicz, *Solitons: Nonlinear Pulses and Beams* (Chapman & Hall, 1997).
- [25] N. R. Pereira and L. Stenflo, *Phys. of Fluids* **20**, 1733 (1977).
- [26] K. Nozaki and N. Bekki, *J. Phys. Soc. of Japan* **53**, 1581 (1984).
- [27] H. Chate and P. Manneville, *Phys. Lett. A* **171**, 183 (1992).